Science of the Total Environment 671 (2019) 765–775

Contents lists available at ScienceDirect

Science of the Total Environment

journal homepage: www.elsevier.com/locate/scitotenv

Sources of humic-like substances (HULIS) in $PM_{2.5}$ in Beijing: Receptor modeling approach

Xinghua Li [a], Kaiqiang Yang [a], Junzan Han [a], Qi Ying [b], Philip K. Hopke [c,d,*]

[a] School of Space and Environment, Beihang University, Beijing 100191, China
[b] Zachry Department of Civil Engineering, Texas A&M University, College Station, TX 77843, USA
[c] Center for Air Resources Engineering and Science, Clarkson University, Potsdam, NY 13699, USA
[d] Department of Public Health Sciences, University of Rochester School of Medicine and Dentistry, Rochester, NY 14642, USA

HIGHLIGHTS

- Sources of PM2.5 and HULIS were apportioned for 2012–2013 using additional variables.
- Eight sources were resolved including residential coal/wood and incinerator emissions.
- Adding gaseous pollutants provided better agreement between PMF and CMAQ results.
- Residential combustion was a major source of PM2.5 and HULIS in Beijing.

GRAPHICAL ABSTRACT

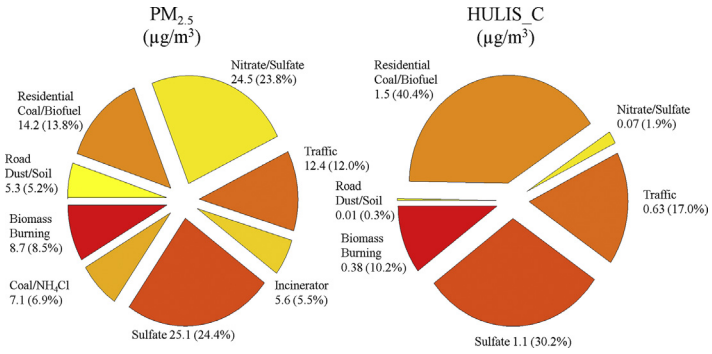

ARTICLE INFO

Article history:
Received 19 December 2018
Received in revised form 21 March 2019
Accepted 22 March 2019
Available online 24 March 2019

Editor: Jianmin Chen

Keywords:
$PM_{2.5}$
HULIS
Source apportionment
PMF
CMAQ

ABSTRACT

Recent work has identified the presence of humic-like substances (HULIS) in ambient fine particulate matter ($PM_{2.5}$) in Beijing, China and that residential coal combustion as well as biomass burning are significant contributors to its presence. These results were based on the characterization of emissions from representative stoves and modeling of the aerosol with the Community Multiscale Air Quality (CMAQ) chemical transport model. The CMAQ source apportionment estimated that residential coal and biofuel burning and secondary aerosol formation were important annual sources of ambient HULIS, contributing 47.1%, 15.1%, and 38.9%, respectively. In this study, chemical composition data including concentrations of water-soluble organic carbon and HULIS across four seasons during 2012–2013 were analyzed with positive matrix factorization (PMF) to provide a complementary source apportionment. The PMF results indicate that the identified sources were Traffic, Biomass Burning, Nitrate/Sulfate, Incineration, Sulfate, Coal Combustion/Ammonium Chloride, Residential Coal/Biofuel Combustion, and Road Dust/Soil with mass contributions (fractions) to $PM_{2.5}$ of 12.35 (10.4%), 8.70 (8.9%), 24.51 (22.4%), 5.64 (7.2%), 25.14 (24.5%), 7.10 (6.2%), 14.18 (15.4%), and 5.33 μg/m^3 (5.0%), respectively. The contributions to the observed HULIS concentrations were 0.63 (10.9%), 0.38 (6.4%), 0.07 (1.7%), 0.00 (0%), 1.12 (28.8%), 0.00 (0%), 1.50 (52.2%), and 0.01 μg/m^3 (0.3%), respectively. These PMF modeling results were in reasonable agreement with the CMAQ values supporting the attribution of significant amounts of primary HULIS to residential coal and biofuel combustion. Currently, efforts are underway in China to replace solid fuel combustion for heating and cooking with natural gas and electricity by 2020. Thus, future studies should be able to see substantial reductions in both $PM_{2.5}$ and HULIS in the near term future.

* Corresponding author at: Center for Air Resources Engineering and Science, Clarkson University, Potsdam, NY 13699, USA.
E-mail address: phopke@clarkson.edu (P.K. Hopke).

https://doi.org/10.1016/j.scitotenv.2019.03.333
0048-9697/

1. Introduction

Humic-like substances (HULIS) are a mixture of water-soluble, relatively high molecular weight organic compounds with structures and properties similar to terrestrial and aquatic humic and fulvic acids (Graber and Rudich, 2006). HULIS are widely distributed in atmospheric samples and can constitute a significant portion of the organic matter and water-soluble organic carbon (WSOC). For example, HULIS were found to constitute 9% to 72% of WSOC (Zheng et al., 2013). HULIS may play important roles in atmospheric processes, such as the formation of clouds as condensation nuclei, ice nuclei, and increased single particle albedo through aerosol hygroscopic growth (Gysel et al., 2004; Dinar et al., 2006; Wang and Knopf, 2011). HULIS play an active role as brown carbon in the radiative transfer and photochemical processes due to its strong light absorption in the ultraviolet range (Hoffer et al., 2006). Its deposition decreases the albedo of ice and snow surfaces (Beine et al., 2011; France et al., 2011, 2012). HULIS can also induce adverse health effects because of their redox-active characteristics (Ghio et al., 1996; Lin and Yu, 2011; Verma et al., 2012).

HULIS concentrations in the ambient aerosol vary over two orders of magnitude, ranging from <0.1 μg/m^3 for background locations to 55 μg/m^3 in polluted urban aerosols (Feczko et al., 2007; Krivácsy et al., 2008; Li et al., 2019). Biomass burning and atmospheric secondary formation have generally been accepted as the important HULIS sources (Zheng et al., 2013; Kuang et al., 2015; Ma et al., 2018; Srivastava et al., 2018). However, residential coal burning was recently suggested as an important primary HULIS source during winter (Tan et al., 2016; Voliotis et al., 2017). Vehicle exhaust is another possible HULIS source although there is uncertainty in the importance of this source (Salma et al., 2007; El Haddad et al., 2009; Lin et al., 2010; Kuang et al., 2015). However, studies on quantitative source apportionment of HULIS are still limited (Kuang et al., 2015; Srivastava et al., 2018; Ma et al., 2018; Li et al., 2018) and thus, a detailed understanding of HULIS sources has not yet been attained.

Beijing, a megacity with over 20 million in population and located in the North China Plain, suffers serious $PM_{2.5}$ pollution, particularly in the winter. Beijing had a vehicle population of up to 5.2 million in 2012. Coal is burned extensively in Beijing and its surrounding areas, especially in the winter when large quantities of coal are consumed for indoor heating as well as cooking. Moreover, a considerable proportion of coal is burned in residential household stoves in rural, suburban, and even some urban areas under poor combustion conditions and without any emission controls (Wang et al., 2016; Liu et al., 2016). Biofuels are also burned in large amounts in these areas for cooking and heating. Source appointment studies indicated that vehicle emissions, coal and biomass burning, and secondary aerosol formation were important sources of ambient $PM_{2.5}$ in Beijing (Zhang et al., 2017; Zíkova et al., 2016; Tao et al., 2016; Zhang et al., 2013). Thus, Beijing provides an ideal location to explore the contribution of a variety of sources to ambient HULIS.

In our previous work, HULIS emitted from residential coal stoves, vehicle exhaust, and residential biofuel burning were measured; and anthropogenic primary emissions of HULIS were estimated (Li et al., 2019). The source-oriented Community Multiscale Air Quality (CMAQ) model was applied to quantitatively determine the source contributions to HULIS in ambient $PM_{2.5}$ in Beijing (Shi et al., 2017; Li et al., 2019). This work provided direct evidence that residential coal burning was a significant source of ambient HULIS in northern China. Vehicle emissions were found to be a negligible contributor to the ambient HULIS. Combining emissions, meteorology, and atmospheric chemical and physical processes, source-oriented models are very powerful in source apportionment. However, uncertainties in emission inventory, meteorology, and atmospheric chemical mechanism could limit the accuracy of results from source-oriented models (Zhang et al., 2017).

To help to better assess source contribution to ambient HULIS, a positive matrix factorization (PMF) source apportionment modeling study using EPA PMF V5 was performed based on 116 ambient $PM_{2.5}$ samples measured in Beijing across the four seasons during 2012–2013. Temperature-resolved carbon fractions and pollutant gases were included in the PMF modeling to help identifying the potential sources. Marmur et al. (2005, 2007) included pollutant gases in their chemical mass balance (CMB) source apportionment of Atlanta $PM_{2.5}$. Kasumba et al. (2009) incorporated pollutant gases in their PMF studies of particle size distributions. Emami and Hopke (2017) specifically examined the utility of adding the gas data to the particle size distribution data and showed that it reduced the rotational ambiguity in the resulting solutions. Incorporating pollutant gases in the PMF studies or not was also explored and compared in this study. The relative contributions of each source to HULIS in the different seasons were estimated. The conditional bivariate probability function (CBPF) was utilized to help identify the likely direction of the PMF identified sources. A feature of this study is the use of the new error analysis tools that were included in EPA PMF V5 (Paatero et al., 2014). HULIS PMF source apportionment results were also compared with our prior study with the source-oriented CMAQ model. Integration of these two models will add confidence to the robustness of source apportionment results for ambient HULIS.

2. Experimental methods

$PM_{2.5}$ samples were collected using a 5-channel Spiral Ambient Speciation Sampler (SASS, Met One Inc., USA) for PM mass, elements, ions, and organic and elemental carbon analysis. In addition, a high-volume aerosol sampler (RFPS-1287-063, Thermo, USA) was operated at a flow rate of 1.13 m^3 min^{-1} to collect $PM_{2.5}$ samples on prebaked quartz filters (with area 417.6 cm^2) for the determination of water-soluble organic carbon (WSOC) and humic-like substances (HULIS). Samples were collected from June 15–30, 2012 and August 10–20, 2012 (summer), September 15 to October 31, 2012 (autumn), from January 5 to February 5, 2013 (winter), and March 4 to April 2, 2013 (spring) on the roof of a building at Beihang University (39°590N, 116°210E) approximately 25 m above ground level. The site is located in urban Beijing, approximately 10 km northwest of the city center and between the 3rd and 4th Ring Roads in northwestern Beijing. This urbanized area is surrounded by educational and residential districts without any major nearby industrial sources (Fig. 1). The sampling procedures were described in detail by Wang et al. (2015). Details of the analytical procedures were provided by Zíkova et al. (2016).

Pollutant gases were measured using standard gas monitors at the Haidian Wanliu air quality observation site. The site is an urban site in Beijing about 5 km from the PM sampling site, and close to 4th Ring Roads in northwestern Beijing. Nitrogen oxides (NO_x) concentrations were measured by a chemiluminescence NO–NO_2–NO_x analyzer (Model 42, Thermo Environmental Instrument Inc., MA, USA). Carbon monoxide (CO), sulfur dioxide (SO_2) and ozone (O_3) concentrations were measured by a CO ambient analyzer (Model 48, Thermo Environmental Instrument Inc., MA, USA), a SO_2 ambient analyzer (Model 43i, Thermo Environmental Instrument Inc., MA, USA) and an O_3 ambient analyzer (Model 49i, Thermo Environmental Instrument Inc., MA, USA), respectively. These data were obtained from the official website of China National Environmental Monitoring Center (http://113.108.142.147:20035/emcpublish/) that operates the gas analyzers and provide their routine calibration and maintenance. Meteorological data including wind speed (WS), temperature, relative humidity (RH) and precipitation were obtained from the China Meteorological Data Service Center (http://data.cma.cn/). A plot of the wind rose for the days on which samples were collected is provided in Fig. S1 of the Supplemental material.

HULIS was isolated using the extraction method developed by Varga et al. (2001) and used in many other studies (Fan et al., 2012; Feczko et al., 2007; Krivácsy et al., 2008; Lin et al., 2010; Lin and Yu, 2011; Nguyen et al., 2014; Salma et al., 2013; Song et al., 2012). The separation procedure is provided in Supporting information Section S1. The WSOC and $HULIS_C$ (HULIS carbon) were determined using a TOC analyzer

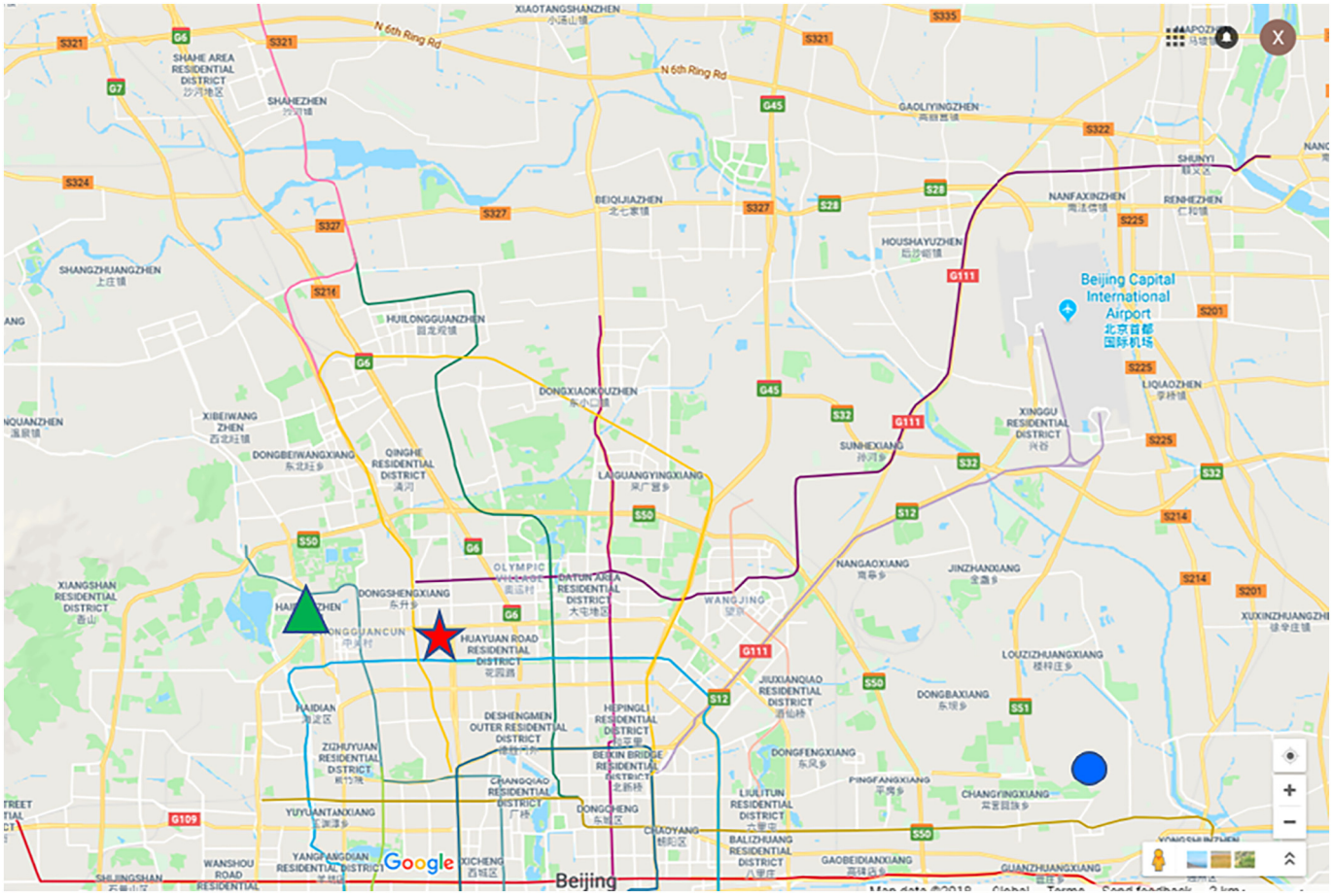

Fig. 1. Location of the PM and gas sampling sites (highlighted with a red star and a green triangle, respectively). The waste incinerators are denoted with blue circles. (For interpretation of the references to colour in this figure legend, the reader is referred to the web version of this article.)
(Maps from https://www.google.com/maps.)

(Shimadzu TOC-Vcph, Japan) based on a combustion-oxidation, non-scattering infrared absorption method. The TOC was determined by subtracting inorganic carbonate (IC) from total carbon (TC): TOC = TC − IC. The data reported were the average results of three measurements. The difference between the total carbon and the WSOC was the water-insoluble carbon (WIC) that would include the water-insoluble organic carbon and the elemental carbon. Mass concentrations of HULIS were obtained from the HULIS carbon content ($HULIS_C$) by multiplying by the factor 1.9 suggested by Lin et al. (2012), Kiss et al. (2002), and Zheng et al. (2013). The average recovery from standard solutions was 89.3 ± 5.3% ($n = 12$), which is comparable to prior studies. The reproducibility was assessed using the relative standard deviation (RSD). RSD for solutions containing 10, 20, 50, and 100 μg/ml of HULIS were 4.7%, 2.3%, 3.4%, and 4.2% ($n = 3$ for each point), respectively (see Supporting Section S1). The detection limit was calculated as 1.09 μg C/ml as described in Supporting Section S1. The distributional characteristics of the resulting data are presented in Table S1.

The datasets with and without the inclusion of the gas concentrations were subjected to positive matrix factorization (PMF) using EPA PMF V5.014. PMF has been described in detail by Hopke (2016) and is now widely used in source apportionment studies. The uncertainties for the PM species were calculated using the approach of Polissar et al. (1998). The uncertainties for the gaseous species were estimated from the manufacturer's reported detection limits and precision (DL + (fractional precision) ∗ value). The number of factors was determined by a combination of the relative values of Q_{robust} and $Q_{theoretical}$, the distributions of the scaled residuals, and the physical/chemical interpretation of the resulting solutions. Rotational ambiguity was explored with a displacement analysis (DISP) and the measurement errors were examined with a bootstrap (BS) analysis (Paatero et al., 2014). The ability to constrain solutions was also used to incorporate information from the measured source profiles for typical residential coal and wood stoves reported by Li et al. (2018) and Dai et al. (2019).

To assist in the identification of the factors, conditional bivariate probability function (CBPF) analyses were applied to each of the factor's contributions. CBPF analysis is discussed in detail by Uria-Tellaetxe and Carslaw (2014). Computation of the CBPF values has been done by using Openair package for R (Carslaw and Ropkins, 2012; Carslaw, 2018).

3. Results and discussion

The prior study of a subset of the present data set by Zíkova et al. (2016) resolved 6 sources. They found source profiles that they identified as secondary sulfate, coal combustion, traffic, secondary nitrate, biomass burning, and soil. In the present study, WIC, WSOC, HULIS_C, the OC and EC fractions, and the pollutant gases were available. Thus, analyses have been made both with and without the inclusion of the gases to ascertain their value in the source apportionment. For the solution with gases, the PM components and the contributions were normalized using the apportioned $PM_{2.5}$ values in the profiles. The gas values were not normalized and presented as provided by the program such that for each factor, the average of each factor contributions (mean g-value) is equal to 1. Thus, the pollutant f-value provides each factor's contribution to the overall average gas concentration.

The gases were included as weak variables since the hourly values had been averaged to provide 24-h values comparable to the PM species

concentrations. Averaging the data loses information (Lioy et al., 1989) and thus, they were included with less weight. Their inclusion without downweighting produced results that were difficult to interpret. The number of factors was varied from 6 to 9. Solutions without the pollutant gases and with them included were explored. Based on the distributions of scaled residuals and the physical interpretability of the resulting solutions, 8 factors were chosen for both data sets (without and with gases). In all cases, there were no DISP swaps and the BS analyses always had at least 80% of the BS solutions adequately correlating with the base case results.

3.1. Source identification

The following factors were resolved for both data sets: Traffic, Biomass Burning, Nitrate/Sulfate, Incineration, Sulfate, Coal Combustion/Ammonium Chloride, Residential Biofuel/Coal Combustion, and Road Dust/Soil. The profiles and contribution plots for the data set that included the pollutant gases are provided in Figs. 2 and 3 while the corresponding plots for the without gas data set are shown in Figs. S2 and S3 in the Supplemental material file. The plots from the CBPF analyses are provided in Fig. 4 for the with gases dataset and in Fig. S4 for the without gases data. For these data analyses, there are the results of the prior CMAQ analyses (Shi et al., 2017; Li et al., 2019) that can serve as a basis of comparison.

3.1.1. Traffic

The traffic factor has high contributions from the OC and EC fractions, WIC, and small amounts of WSOC and HULIS_C. There are small concentrations of Fe, Mn, Pb, Br, and Cl^-. For the with-gases results, there are high contributions of NO, NO_2, SO_2, and some CO. However, nitrate was zero and typically some nitrate is observed when there are

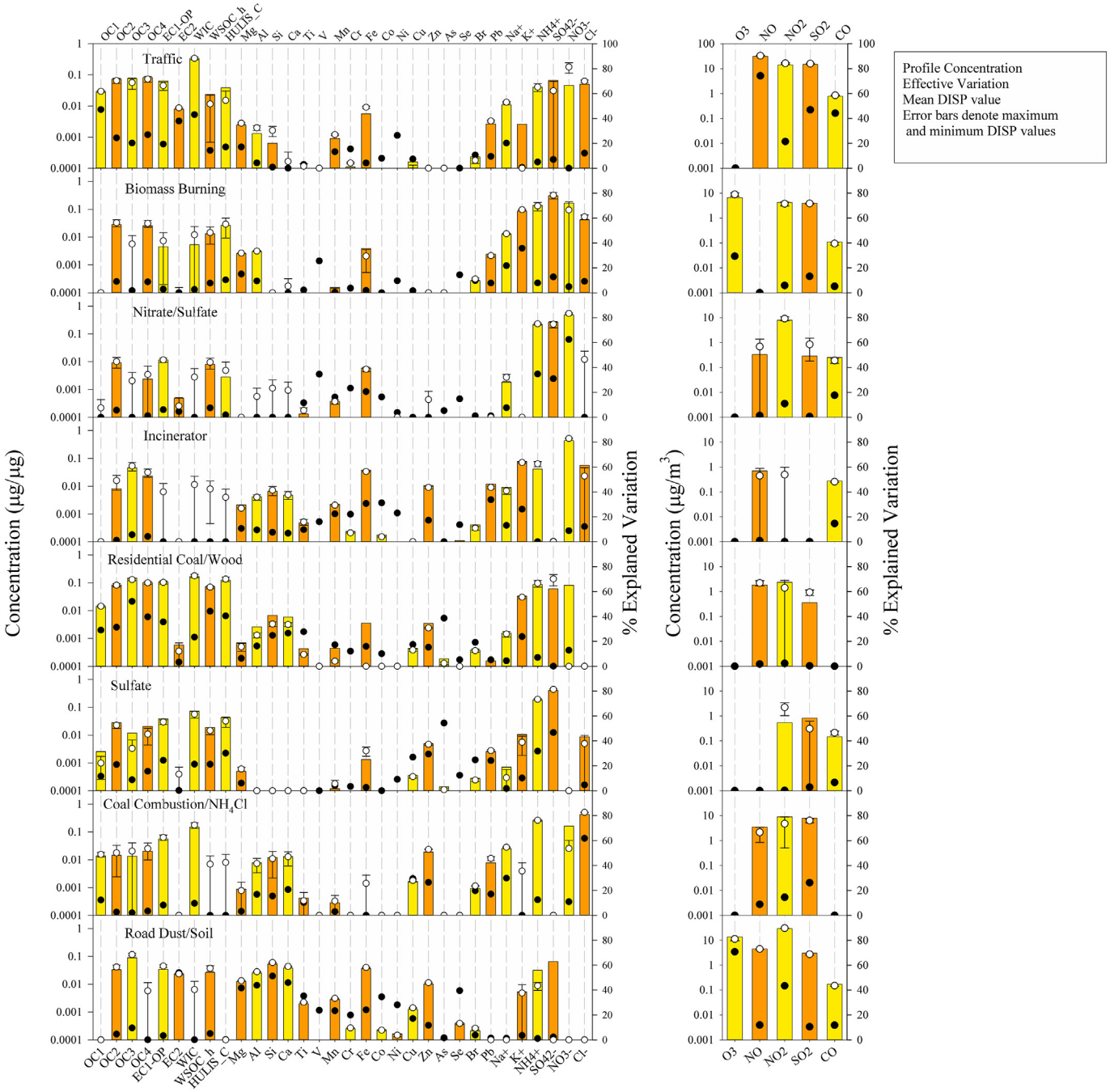

Fig. 2. Profiles of the sources resolved by the constrained PMF analysis from the data collected during 2012–2013.

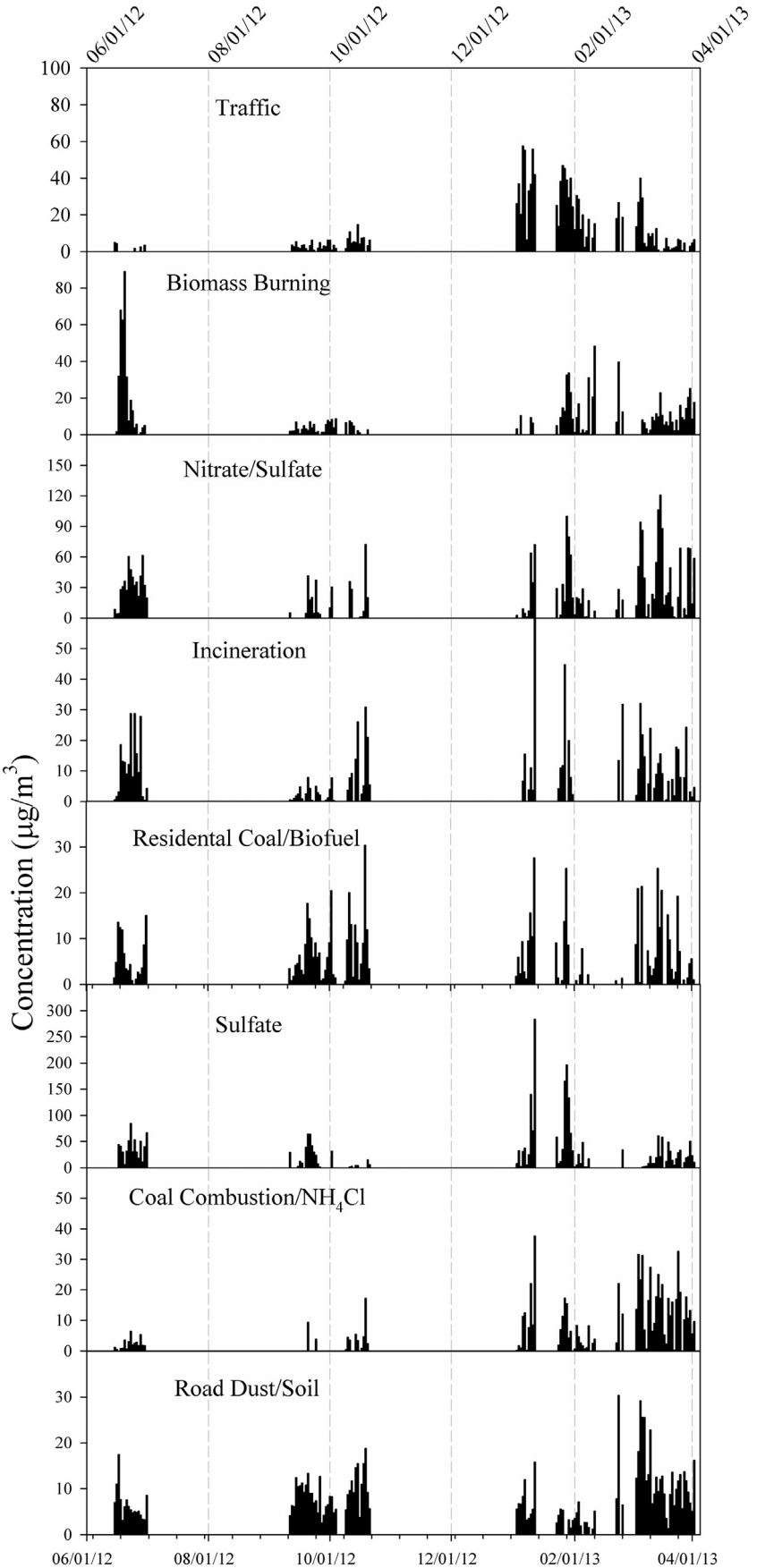

Fig. 3. Time series of contributions of the factors resolved using the constrained PMF analysis including the pollutant gases.

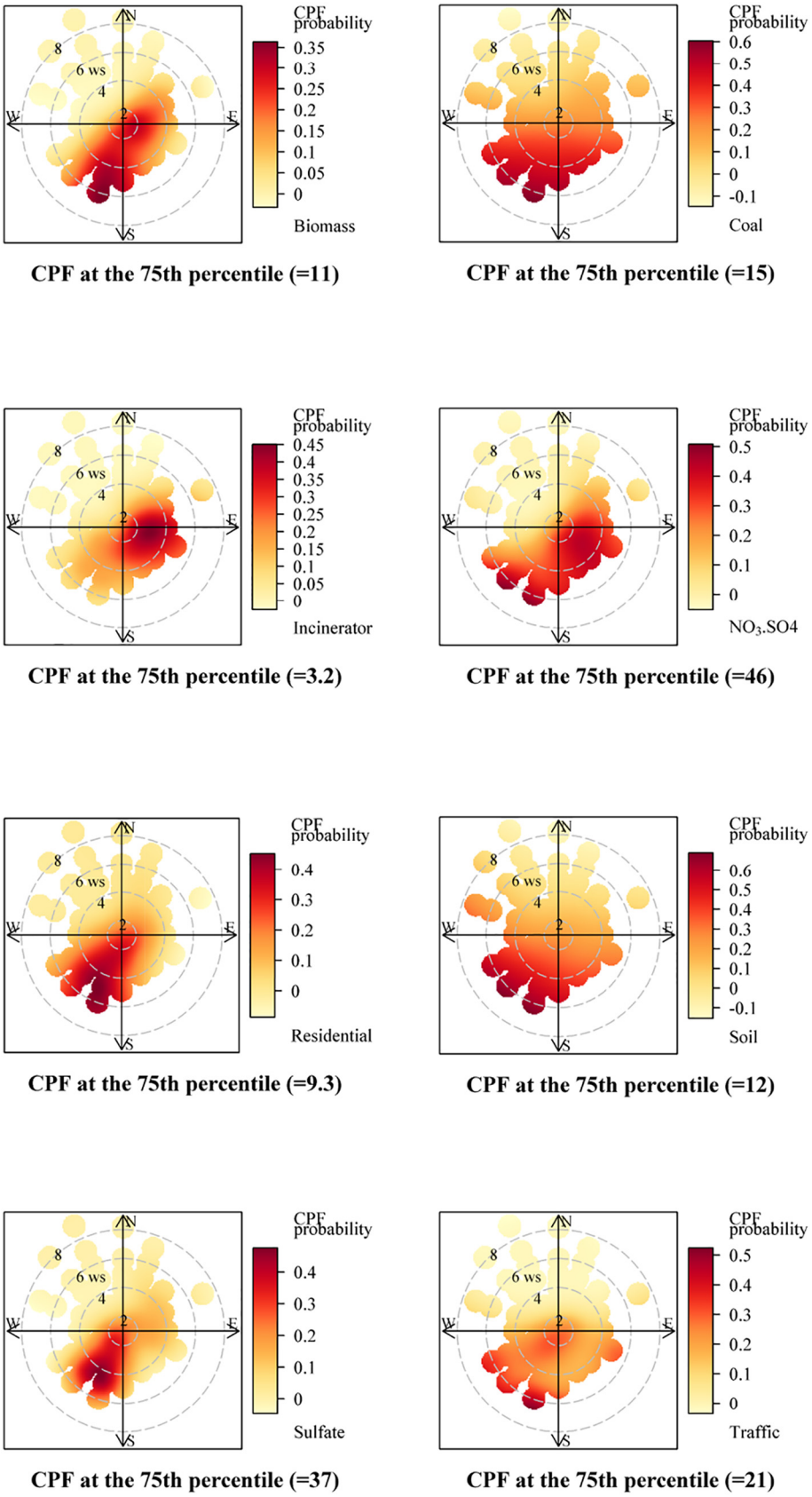

Fig. 4. CBPF plots for each of the 8 factors extracted from the dataset including the pollutant gases. Wind speeds are in m/s. Values in the parentheses are the 75th percentile values in μg/m^3.

diesel vehicle emissions (Squizzato et al., 2018). Thus, in the constrained run, the nitrate was maximally pulled upward. Additional constraints were also placed on elements of the Residential Coal/biofuel profile and will be discussed below. The constraints increased the Q-value by 0.82% and again, there were no DISP swaps and all of the BS runs had at least 80% agreement with the base case values. The $PM_{2.5}$

mass contributions from the solutions with and without the pollutant gases (Figs. 3 and S3) are fairly similar throughout the year with somewhat higher values during the winter and early spring when mixed layer heights and wind speeds are low resulting in poor dispersion conditions. The with-gases solution has higher WIC and lower WSOC and HULIS_C and more ammonium and sulfate than in the without-gas profile. In general, the DISP intervals in the with-gas results are smaller suggesting less rotational ambiguity in line with the results of Emami and Hopke (2017) showing that the addition of pollutant gases produced smaller DISP intervals in the analysis of particle size distribution data. The CBPF plots (Figs. 4 and S4) show the highest traffic coming from the SW direction, which is the major prevailing wind direction from a large area of the city such that significant traffic aerosol could be transported to the sampling site.

3.1.2. Biomass burning

This factor had the highest contribution to K^+ with some carbonaceous material including WSOC and HULIS_C. Potassium is the commonly used marker element for biomass combustion and it is also known that biomass combustion produces water-soluble carbonaceous materials as observed by Li et al. (2019). Kumar et al. (2018) report that agricultural burning in India produced a strong correlation of HULIS-C with K^+ ($r^2 > 0.80$) and significant day-night variability of the HULIS-C/WSOC ratio. Air-mass back trajectories showed transport of pollutants from the upwind Indo-Gangetic Plain and thus, suggesting biomass burning emissions and secondary transformations as important sources of HULIS in this region. High-loadings of atmospheric PM_{10} (as high as 440 μg m^{-3}) with significant contributions of water-soluble organic matter (WSOC/OC: ~0.40–0.80) were observed during wintertime.

There is also ammonium sulfate in this profile and contributes 6 μg/m^3 to the summer $PM_{2.5}$ concentrations. The chemical reactions within the biomass burning aerosol are known to produce significant quantities of oxidative species including ozone (Mao et al., 2013). Thus, any SO_2 entrained into the biomass burning aerosol will be readily oxidized to ammonium sulfate and will covary with K^+.

High contributions of the biomass burning source were observed in the summer 2012 samples and low to moderate values in winter and spring 2013 suggesting that this source largely represents agricultural burning analogous to the CMAQ open biomass burning source. It was the major source of HULIS-C for the summer samples. The CBPF plots (Figs. 4 and S4) show a strong SSW direction at higher wind speeds suggesting this source is at a distance and its impact comes from transported PM.

3.1.3. Nitrate/sulfate

One of the mechanisms suggested to explain the high concentration of winter sulfate in Beijing is one in which SO_2 partitions into cloud or fog droplets and is then oxidized by dissolved NO_2 in fog droplets at a typical haze-fogwater pH of 5.6 (Cheng et al., 2016). The heterogeneous reaction of SO_2 on the particle surfaces was also suggested to be important based on the modeling done by Xue et al. (2014, 2016), Hu et al. (2016), Shi et al. (2017) and Qiao et al. (2018). Li et al. (2018) suggested that observations of high nitrate and sulfate concentrations supported the application of this mechanism. In both sets of solutions, a nitrate/sulfate factor is observed and contributes the most nitrate as well as significant sulfate (Table S2). This factor is high in the winter and early spring with spring being somewhat higher than winter as reported by Li et al. (2019) when there would be warmer temperatures and greater photochemical activity. The CBPF plots show multiple directions from the south with the highest probability direction being SE under light winds.

3.1.4. Incineration

There are several municipal solid waste incinerators in the vicinity of the sampling site. One is located approximately 20 km to the southeast of the monitoring site (Fig. 1). This factor was not resolved in the previous analysis (Zíkova et al., 2016). However, they suggested that incineration might have been intermixed with the biomass burning factor because of the presence of Fe and Zn. The factor also has a substantial K^+ contribution that would come from burning paper and other biomass such as food waste. There is a significant Cl^- contribution that was often seen in incinerator emissions from the combustion of PVC plastic (Greenberg, 1976). It also contributes nitrate. It appears to be a source of CO and a possible source of NO since the NO value has a large DISP interval. This factor contributed relatively little mass, but its highest mass contributions occurred in the winter period. The CBPF plots (Figs. 4 and S4) shows that the plant to the southeast that has the substantial influence. The SE directionality of this point source has a degree of overlap with the Nitrate/Sulfate source. High-temperature combustion in the incinerator could be a local source of oxidative species, nitrate, and water vapor that could facilitate the liquid phase reactions.

3.1.5. Residential coal/biofuel combustion

In many upwind provinces (e.g., Hebei, Shanxi, Shandong), much of the space heating and cooking continued to be done with lump or briquette coal and biofuel as previously seen in Xi'an (Dai et al., 2018) and Lanzhou (Tan et al., 2016). Li et al. (2019) have measured emissions from coal stoves as has Dai et al. (2019) and both have found significant emissions of sulfate and organic carbon. Li et al. (2019) have also reported the emission of primary HULIS. Tan et al. (2016) suggested that residential coal combustion was a significant source of HULIS in Lanzhou. This source profile has the highest explained variation for HULIS_C in this analysis. It also has a significant K^+ contribution and wood and agricultural wastes are also burned for heating and cooking. Thus, this profile is assigned to residential solid fuel combustion with its highest values during the heating season but continuing throughout the year since these stoves are also used for cooking. However, there is no sulfate associated with this factor in spite of the findings of Dai et al. (2019) that coal combustion in typical residential stoves was a major source of primary sulfate. There is a moderately large DISP interval suggesting that it could be constrained to include a significant sulfur concentration. This problem can be resolved in the consideration of the next factor.

3.1.6. Sulfate

This factor provides the majority of the sulfate (Table S2) and a corresponding amount of ammonium. It also includes some OC and EC as is typically seen in a sulfate factor (e.g., Kim et al., 2004; Kim and Hopke, 2004a, 2004b). However, contrary to most locations, the sulfate factor contributed the most mass in winter whereas in most other locations, sulfate peaks in the summer when photochemical activity is the highest. In the winter in Beijing, temperatures are near 0 °C, and there is diminished light intensity because of the high PM concentrations and fogs. In addition, the highest NO_x concentrations were observed in the winter (Table S3), and they would serve as a substantial reaction sink for hydroxyl radicals given their large rate constants. Thus, homogeneous secondary formation reactions on sulfate particles are limited. It is likely that aqueous phase oxidation by O_2 with Mn/Fe catalysis either in cloud/fog drop or in the liquid layers on particle surfaces at high relative humidity is an important pathway for sulfate formation.

However, the sulfate is also present as the result of direct emissions from residential coal stoves based on the source measurements made by Dai et al. (2019). It is a common problem in factor analysis that when there is a factor that essentially represents a single species (or in this case both ammonium and sulfate), it will tend to take the variance of those species from the other factors (for example, see Lee et al., 2006). Such a result was observed in Seattle, WA by Kim and Hopke (2008) for primary sulfate emitted from marine diesel engines. In the examination of the g-space plot of sulfate against the residual oil source (marine diesel engines) (Kim and Hopke, 2008), strong edges with the same slopes were seen for each of the three sampling sites affected by ship emissions. Fig. 5 shows the g-space plot for Residential

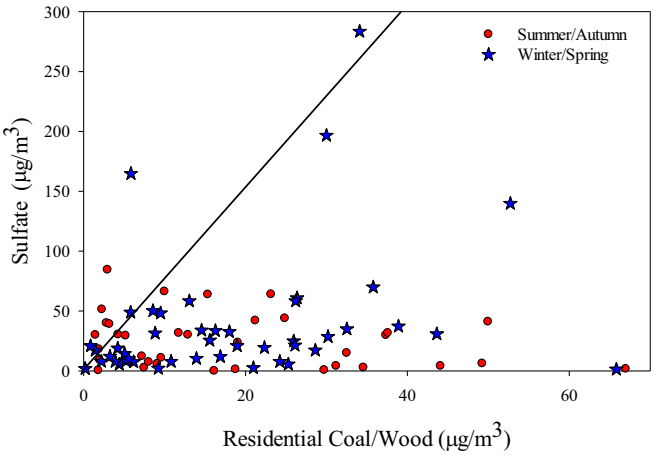

Fig. 5. G-space plot of the Sulfate factor against Residential Coal/Wood.

Coal/Wood against the Sulfate factor. There is an edge that can be observed for the winter/spring data even though there is an anomalous point, but the edge does not exist for the summer/autumn data. An edge represents the correlation between two sources (Henry, 2003; Begum et al., 2005). Thus, in addition to the sulfate that was directly attributed to Residential Coal/Wood (1.35 μg/m^3 in winter and 2.21 μg/m^3 in the spring), an additional part of the observed winter sulfate is due to direct emissions from residential combustion as observed by Li et al. (2019) and Dai et al. (2019). The CMAQ estimation was that for winter, Residential Coal contributed 4.89 μg/m^3 while in spring, 1.55 μg/m^3 could be attributed to this source (Table S4 derived from the results of Shi et al. (2017) and Li et al. (2019).

3.1.7. Coal combustion/NH_4Cl

High-temperature coal combustion is a major energy source in China with a large fraction of the electricity generating capacity being coal-fired power plants. It is also used for some district space heating. In Beijing, substitution of natural gas for the coal has been actively promoted in recent years. However, in the winter of 2013, there would still be space heating with high-temperature coal combustion. Previous work has identified that coal burned in these plants is high in chlorine. Yu et al. (2013) showed the Cl is strongly associated with coal combustion in Beijing based on laboratory analysis of coal combustion smoke made by Zheng et al. (2005). There are tight DISP bounds on both the ammonium and chloride in this profile suggesting the HCl that would be emitted by the coal combustion has reacted with the ambient ammonia to form ammonium chloride. Li et al. (2019) also suggested that Cl· radicals could form and participate in the formation of winter secondary aerosol. The contributions for this source are highest in the winter and early spring suggesting that building heating is likely more important than power plant emissions. Any coal-fired power plant with a flue-gas desulfurization system would also have most of the HCl removed from the effluent.

3.1.8. Road dust/soil

The last factor has high contributions to the crustal elements (Al, Si, Ca, Ti) and several transition metals that would be associated with brake wear, tire wear, and ablation of mufflers. Although there are moderate concentrations of ammonium and sulfate, their DISP intervals extend to zero and their contributions to their explained variations are very small. Thus, these species can be ignored for this factor. Its contributions were highest in the spring period when desert dust episodes affect the Beijing region, so this factor includes both resuspended road dust and atmospherically transported soil. The CBPF plots point to the SW of the sampling site with the high probabilities being for periods of higher wind speeds. Higher wind speeds would aid in the transport of both resuspended road dust as well as marking the spring periods when there can be substantial transport of dust from the western deserts.

3.2. Comparison of PMF and CMAQ results

3.2.1. Comparison of the PMF solutions

In the present study, two solutions of 8 factors were obtained for the data with and without the inclusion of the pollutant gases. In addition, Ma et al. (2018) report a PMF analysis of data from 66 samples collected between March 2012 and March 2013 on the campus of Peking University that is 3 km west-northwest of the Beihang University site. They only report 13 species that did not include OC and EC fractions, nitrate, or trace elements. Thus, they only resolved 5 sources: coal combustion, biomass burning, waste incineration, vehicle emissions, and secondary aerosol formation. Since their "secondary" aerosol was identified by the presence of sulfate, their results are similar in that this source was the major contributor to the observed HULIS_C. As noted above, the sulfate was partly related to primary emissions from coal combustion

Table 1
Mean contributions (mass and fractional) of the sources to the observed mass concentrations.

Mean mass contributions (μg m^{-3})									
Without gases	$PM_{2.5}$	WIC	WSOC	HULIS_C	With gases	$PM_{2.5}$	WIC	WSOC	HULIS_C
Biomass	7.80	0.00	0.33	0.65	Biomass	9.16	0.05	0.12	0.24
Coal	9.86	0.63	0.00	0.00	Coal	6.42	0.95	0.00	0.00
Incinerator	2.19	0.00	0.00	0.00	Incinerator	7.40	0.00	0.00	0.00
NO_3^-/SO_4^{2-}	27.48	0.00	0.25	0.19	NO_3^-/SO_4^{2-}	23.04	0.00	0.19	0.06
Residential coal/wood	6.21	0.00	0.74	1.17	Residential coal/wood	15.92	2.70	1.17	1.97
Road dust/soil	8.40	0.19	0.15	0.00	Road dust/soil	5.13	0.00	0.14	0.00
SO_4^{2-}	26.96	2.84	0.18	0.61	SO_4^{2-}	25.29	1.83	0.48	1.09
Traffic	14.36	5.78	0.70	1.14	Traffic	10.71	3.62	0.25	0.41
Mean % contribution									
Without gases	$PM_{2.5}$	WIC	WSOC	HULIS_C	With gas	$PM_{2.5}$	WIC	WSOC	HULIS_C
Biomass	7.56	0.00	13.85	17.29	Biomass	8.89	0.54	5.16	6.44
Coal	9.55	6.63	0.00	0.00	Coal	6.23	10.41	0.00	0.00
Incinerator	2.12	0.00	0.00	0.00	Incinerator	7.18	0.00	0.00	0.00
NO_3^-/SO_4^{2-}	26.61	0.00	10.76	5.02	NO_3^-/SO_4^{2-}	22.35	0.00	7.96	1.72
Residential coal/wood	6.01	0.00	31.39	31.09	Residential coal/wood	15.44	29.53	49.91	52.19
Road dust/soil	8.13	2.01	6.49	0.00	Road dust/soil	4.98	0.00	5.75	0.00
SO_4^{2-}	26.11	30.09	7.70	16.23	SO_4^{2-}	24.54	20.01	20.44	28.77
Traffic	13.90	61.27	29.82	30.37	Traffic	10.39	39.52	10.77	10.89

Table 2
Correlation matrix for the time series of contributions from the two data sets.

		With gases solution							
		Biomass	Coal	SO_4^{2-}	Incinerator	Traffic	NO_3^-/SO_4^{2-}	Residential	Road dust
Without gases solution	Traffic	0.085	0.446	0.145	0.265	**0.855**	0.159	0.721	−0.464
	Biomass	**0.918**	0.160	0.306	0.353	0.202	0.444	0.398	−0.433
	NO_3^-/SO_4^{2-}	0.433	0.489	0.481	0.429	0.114	**0.978**	0.406	−0.188
	Incinerator	0.047	0.485	0.734	**0.963**	0.289	0.464	0.120	−0.271
	SO_4^{2-}	0.147	0.400	**0.973**	0.500	0.410	0.506	0.031	−0.217
	Coal	0.089	**0.975**	0.479	0.640	0.426	0.562	0.417	−0.092
	Residential	0.054	0.454	0.546	0.279	0.100	0.452	**0.612**	−0.002
	Road dust	−0.082	0.485	−0.147	0.237	0.005	0.156	0.567	**0.554**

Bolded entries indicate values greater than 0.5.

in residential stoves in winter. They also identify biomass burning based on organic markers and thus, it may in part, represent the wood combustion in residential stoves.

To compare our two solutions with and without the inclusion of the pollutant gases, a correlation matrix was developed between the contribution time series. These results are presented in Table 2. For all of the 8 factors except residential coal/biofuel and road dust, there are high correlations between the two solutions. Thus, the relative concentrations of the two solutions are generally very similar. For residential coal/biofuel and road dust/soil, the correlations are much lower. These results would suggest that these two sources may be correlated because of other factors such as seasonality or meteorology. Their CBPF plots have significant similarities in terms of both wind speed and direction. Thus, the transport process may result in the observed covariance and it is the presence of the gases in the one solution that changes the contributions from these two sources in the two solutions.

The mean mass contributions in μg/m^3 and the % contributions to the explained variation for both datasets are presented in Table 1. For most of the factors, the $PM_{2.5}$ contributions are similar between the two solutions. The Incinerator contribution for the with-gases solution is more than twice that for the without-gases results. Residential Coal/biofuel combustion doubles while the Coal factor and Road Dust/Soil are reduced by one-third. The other differences are relatively small and likely within the level of uncertainty that would be expected in such apportionments.

3.2.2. Comparison the PMF solutions with the CMAQ modeling

Li et al. (2019) examined the CMAQ results only for those days on which samples were collected at Beihang University. The CMAQ modeled Residential biofuel burning, Residential coal burning, Transportation, Industries, Biomass open burning, and Secondary processes. Fig. 6 presents a comparison of the $PM_{2.5}$ and HULIS contributions estimated by CMAQ and the two PMF analyses for each of the jointly estimated sources. The PMF Nitrate/Sulfate source cannot be compared to the CMAQ results since the CMAQ secondary modeling was run primarily to explore the sources of HULIS and not to fully reproduce the $PM_{2.5}$ mass concentrations. Thus, no comparable source was included in the CMAQ results. Power and Industry in the CMAQ analysis both represent high-temperature coal combustion, and thus, they were summed for comparison with the PMF Coal Combustion/NH_4Cl source. CMAQ Residential coal burning and Residential biofuel burning were summed to compare with the PMF Residential Coal/biofuel combustion factor.

The differences among the CMAQ and PMF results for Traffic may result from an underestimation by CMAQ. The 2013 emissions inventory used for the CMAQ modeling only included tailpipe emissions and did not include the other direct emissions such as brake and tire wear (Padoan and Amato, 2018). In addition, the PMF results for Traffic may have also included some secondary aerosol formation resulting from the tailpipe emissions such as ammonium nitrate.

CMAQ produced many zero values for Biomass open burning and appears to have underestimated the contributions from that source. Open biomass burning was estimated using the FINN dataset from the National Center for Atmospheric Research (NCAR) (Wiedinmyer et al., 2011). Although the FINN inventory is global, its results may not fully reflect the agricultural burning conditions in China in 2012–2013.

The agreement among the other sources is reasonable given the uncertainties in both the CMAQ and PMF analyses. CMAQ estimated that Residential biofuel burning, Residential coal burning, Transportation, Industries, Biomass open burning, and Secondary processes contributed 47.1 ± 6.5, 15.1 ± 2.9, 2.0 ± 0.3, 1.3 ± 0.3, 1.7 ± 0.7, and 38.9 ± 9.1% of the HULIS present the atmosphere. Thus, combining the residential sources would suggest that 62.2% of the HULIS was from these sources (Li et al., 2019). The PMF results in Table 1 suggest that for the data including the gases, 52.2% of the HULIS on the days when measurements

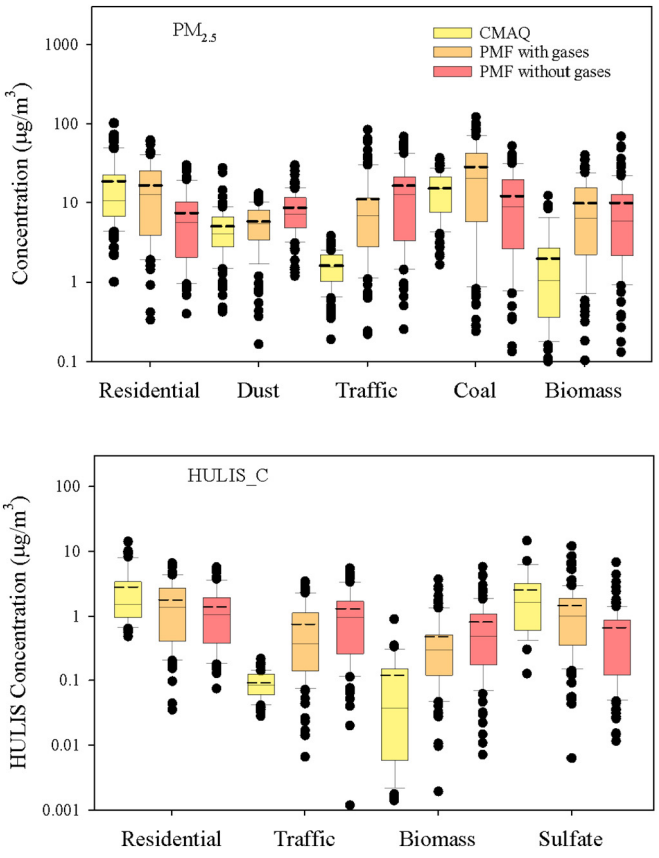

Fig. 6. Comparison of the contributions of the sources to the Beijing $PM_{2.5}$ (top) and HULIS (bottom) concentrations on the days when samples were collected. The PMF Residential included Residential Coal/Wood while CMAQ Residential was the sum of Residential Coal and Residential Wood. The CMAQ Coal was the sum of Power and Industry. The CMAQ Secondary HULIS (bottom) was compared with the HULIS contributions from the Sulfate factor.

were made was from residential combustion sources while the without gases solution only included 31.1%. The Sulfate factor provided 28% of the HULIS and <2% from the Nitrate/Sulfate factor for the with-gases and less from these sources from the without-gases data solution. Thus, assuming that the sulfate partly originates from residential stoves, the combination of the two factors from the with-gases solution (Sulfate and Residential Coal/Wood) would contribute HULIS-C in an amount comparable to that observed in the CMAQ results.

It appears that residential heating and cooking with solid fuels represents a serious air pollution problem because of their direct emission of organic carbon that has significant secondary characteristics and primary sulfate. The Government of China has recognized this problem and undertaken a program to replace all of the old residential solid fuel stoves with either natural gas or electric units. In 2017, the program began with a plan to convert 4 million homes to natural gas (Huang, 2017) including 126,000 stoves in the Beijing area (Xinhua, 2017). However, the rapid addition of this much demand caused shortages of natural gas resulting in some households with no heat. However, the plan is to switch >1 million addition homes this year from coal (Reuters, 2018). Such large-scale changes in emissions should be readily observable in future studies and substantial reductions would confirm the results of this study in terms of the role of residential heating and cooking in creating high pollution periods in the winter of 2012–13.

4. Conclusions

The inclusion of gaseous pollutants with the enhanced suite of chemical constituents in $PM_{2.5}$ has permitted an analysis that provides good agreement with the results of the source-oriented CMAQ modeling. Thus, it is suggested that there be more exploration of the use of combined particulate and gases data in future source apportionment studies. It can also be concluded that residential solid fuel combustion (coal and biomass) contributes significantly to the $PM_{2.5}$ concentrations in Beijing in terms of both secondary-like organic carbon (WSOC and HULIS) and sulfate. Since the Government of China is now undertaking an extensive program of replacing the solid fuel stoves, future accountability studies will be needed to assess the effectiveness of the replacement of solid fuels with natural gas and electricity since the results presented here and in Li et al. (2019) and Dai et al. (2018, 2019) would suggest that substantial reductions in winter concentrations should be expected.

This work also sees potential evidence supporting the hypothesized liquid phase oxidation mechanism for the winter formation of sulfate through reactions with nitrogenous species in fog and cloud water in addition to the aqueous phase oxidation through Fe/Mn + O_2 pathway and heterogeneous reactions. Further study of this reaction pathway is needed to fully understand its importance in winter time pollution episodes as well as identifying the appropriate control measures to mitigate this process.

Acknowledgments

This work was supported by the National Natural Science Foundation of China (Grant No. 41575119, 41275121).

Appendix A. Supplementary data

Supplementary data to this article can be found online at https://doi.org/10.1016/j.scitotenv.2019.03.333.

References

Begum, B.A., Kim, E., Jeong, C.H., Lee, D.W., Hopke, P.K., 2005. Evaluation of the potential source contribution function using the 2002 Quebec forest fire episode. Atmos. Environ. 39, 3719–3724.

Beine, H., Anastasio, C., Esposito, G., Patten, K., Wilkening, E., Domine, F., Voisin, D., Barret, M., Houdier, S., Hall, S., 2011. Soluble, light absorbing species in snow at Barrow, Alaska. J. Geophys. Res. 116, D00R05.

Carslaw, D.C., 2018. Package "openair". Tools for the analysis of air pollution data. Available from. http://davidcarslaw.github.io/openair/, Accessed date: February 2018.

Carslaw, D.C., Ropkins, K., 2012. Openair - an R package for air quality data analysis. Environ. Model. Softw. 27–28, 52–61.

Cheng, Y., Zheng, G., Wei, C., Mu, Q., Zheng, B., Wang, Z., Gao, M., Zhang, Q., He, K., Carmichael, G., Pöschl, U., Su, H., 2016. Reactive nitrogen chemistry in aerosol water as a source of sulfate during haze events in China. Sci. Adv. 2, e1601530.

Dai, Q., Bi, X., Liu, B., Li, L., Ding, J., Song, W., Bi, S., Schulze, B., Song, C., Wu, J., Zhang, Y., Feng, Y., Hopke, P.K., 2018. Chemical nature of PM2.5 and PM10 in Xi'an, China: insights into primary emissions and secondary particle formation. Environ. Pollut. 240, 155–166.

Dai, Q., Bi, X., Song, W., Li, T., Liu, B., Ding, J., Xua, J., Song, C., Yang, N., Schulze, B.C., Zhang, Y., Feng, Y., Hopke, P.K., 2019. Residential coal combustion as a source of primary sulfate in Xi'an, China. Atmos. Environ. 196, 66–76.

Dinar, E., Taraniuk, I., Graber, E.R., Katsman, S., Moise, T., Anttila, T., Mentel, T.F., Rudich, Y., 2006. Cloud condensation nuclei properties of model and atmospheric HULIS. Atmos. Chem. Phys. 6, 2465–2481.

El Haddad, I., Marchand, N., Dron, J., Temime-Roussel, B., Quivet, E., Wortham, H., Jaffrezo, J.-L., Baduel, C., Voisin, D., Besombes, J., Gille, G., 2009. Comprehensive primary particulate organic characterization of vehicular exhaust emissions in France. Atmos. Environ. 43, 6190–6198.

Emami, F., Hopke, P.K., 2017. Effect of adding variables on rotational ambiguity in positive matrix factorization solutions. Chemom. Intell. Lab. Syst. 162, 198–202.

Fan, X.J., Song, J.Z., Peng, P.A., 2012. Comparison of isolation and quantification methods to measure humic-like substances (HULIS) in atmospheric particles. Atmos. Environ. 60, 366–374.

Feczko, T., Puxbaum, H., Kasper-Giebl, A., Handler, M., Limbeck, A., Gelencsér, A., Pio, C., Preunkert, S., Legrand, M., 2007. Determination of water and alkaline extractable atmospheric humic-like substances with the TU Vienna HULIS analyzer in samples from six background sites in Europe. J. Geophys. Res. 112, D23S10.

France, J.L., King, M.D., Frey, M.M., Erbland, J., Picard, G., Preunkert, S., MacArthur, A., Savarino, J., 2011. Snow optical properties at Dome C (Concordia), Antarctica, implications for snow emissions and snow chemistry of reactive nitrogen. Atmos. Chem. Phys. 11, 9787–9801.

France, J.L., Reay, H.J., King, M.D., Voisin, D., Jacobi, H.W., Domine, F., Beine, H., Anastasio, C., MacArthur, A., Lee-Taylor, J., 2012. Hydroxyl radical and NOx production rates, black carbon concentrations and light-absorbing impurities in snow from field measurements of light penetration and nadir reflectivity of onshore and offshore coastal Alaskan snow. J. Geophys. Res. 117, D00R12.

Ghio, A.J., Stonehuerner, J., Pritchard, R.J., Piantadosi, C.A., Quigley, D.R., Dreher, K.L., Costa, D.L., 1996. Humic-like substances in air pollution particulates correlate with concentrations of transition metals and oxidant generation. Inhal. Toxicol. 8, 479–494.

Graber, E.R., Rudich, Y., 2006. Atmospheric HULIS: how humic-like are they? A comprehensive and critical review. Atmos. Chem. Phys. 6, 729–753.

Greenberg, R.R., 1976. A Study of Trace Elements Emitted on Particles From Municipal Incinerators. (Ph.D. Thesis). University of Maryland.

Gysel, M., Weingartner, E., Nyeki, S., Paulsen, D., Baltensperger, U., Galambos, I., Kiss, G., 2004. Hygroscopic properties of water-soluble matter and humic-like organics in atmospheric fine aerosol. Atmos. Chem. Phys. 4, 35–50.

Henry, R.C., 2003. Multivariate receptor modeling by N-dimensional edge detection. Chemom. Intell. Lab. Syst. 65, 179–189.

Hoffer, A., Gelencser, A., Guyon, P., Kiss, G., Schmid, O., Frank, G.P., Artaxo, P., Andreae, M.O., 2006. Optical properties of humic-like substances (HULIS) in biomass-burning aerosols. Atmos. Chem. Phys. 6, 3563–3570.

Hopke, P.K., 2016. Review of receptor modeling methods for source apportionment. J. Air Waste Manage. Assoc. 66, 237–259.

Hu, J., Chen, J., Ying, Q., Zhang, H., 2016. One-year simulation of ozone and particulate matter in China using WRF/CMAQ modeling system. Atmos. Chem. Phys. 16, 10333–10350.

Huang, E., 2017. China's putting the brakes on coal for heating millions of homes this winter. https://qz.com/1093898/chinas-putting-the-brakes-on-coal-for-heating-millions-of-homes-this-winter/, Accessed date: 2 March 2019.

Kasumba, J., Hopke, P.K., Chalupa, D.C., Utell, M.J., 2009. Comparison of sources of submicron particle number concentrations measured at two sites in Rochester, N. Y. Sci. Total Environ. 407, 5071–5084.

Kim, E., Hopke, P.K., 2004a. Source apportionment of fine particles at Washington, DC utilizing temperature resolved carbon fractions. J. Air Waste Manage. Assoc. 54, 773–785.

Kim, E., Hopke, P.K., 2004b. Improving source identification of fine particles in a rural northeastern U.S. area utilizing temperature resolved carbon fractions. J. Geophys. Res. 109, D09204.

Kim, E., Hopke, P.K., 2008. Source characterization of ambient fine particles at multiple sites in the Seattle area. Atmos. Environ. 42, 6047–6056.

Kim, E., Hopke, P.K., Edgerton, E.S., 2004. Improving source identification of Atlanta aerosol using temperature resolved carbon fractions in positive matrix factorization. Atmos. Environ. 38, 3349–3362.

Kiss, G., Varga, B., Galambos, I., Ganszky, I., 2002. Characterization of water-soluble organic matter isolated from atmospheric fine aerosol. J. Geophys. Res. 107, 8339.

Krivácsy, Z., Kiss, G., Ceburnis, D., Jennings, G., Maenhaut, W., Salma, I., Shooter, D., 2008. Study of water-soluble atmospheric humic matter in urban and marine environments. Atmos. Res. 87, 1–12.

Kuang, B.Y., Lin, P., Huang, X.H.H., Yu, J.Z., 2015. Sources of humic-like substances in the Pearl River Delta, China: positive matrix factorization analysis of $PM_{2.5}$ major components and source markers. Atmos. Chem. Phys. 15, 1995–2008.

Kumar, V., Rajput, P., Goel, A., 2018. Atmospheric abundance of HULIS during wintertime in Indo-Gangetic Plain: impact of biomass burning emissions. J. Atmos. Chem. 2018. https://doi.org/10.1007/s10874-018-9381-4.

Lee, J.H., Hopke, P.K., Turner, J.R., 2006. Source identification of airborne PM2.5 at the St. Louis-Midwest Supersite. J. Geophys. Res. 111, D10S10.

Li, H., Duan, F., Ma, Y., He, K., Zhu, L., Ma, T., Ye, S., Yang, S., Huang, T., Kimoto, T., 2018. Case study of spring haze in Beijing: characteristics, formation processes, secondary transition, and regional transportation. Environ. Pollut. 242, 544–554.

Li, X., Han, J., Hopke, P.K., Hu, J., Shu, Q., Chang, Q., Ying, Q., 2019. Quantifying primary and secondary humic like substances in urban aerosol based on emission source characterization and a source-oriented air quality model. Atmos. Chem. Phys. 19, 2327–2341.

Lin, P., Yu, J.Z., 2011. Generation of reactive oxygen species mediated by humic-like substances in atmospheric aerosols. Environ. Sci. Technol. 45, 10362–10368.

Lin, P., Huang, X.F., He, L.Y., Yu, J.Z., 2010. Abundance and size distribution of HULIS in ambient aerosols at a rural site in South China. J. Aerosol Sci. 41, 74–87.

Lin, P., Rincon, A.G., Kalberer, M., Yu, J.Z., 2012. Elemental composition of HULIS in the Pearl River Delta Region, China: results inferred from positive and negative electrospray high resolution mass spectrometric data. Environ. Sci. Technol. 46, 7454–7462.

Lioy, P.J., Zelenka, M.P., Cheng, M.-D., Reiss, N.M., Wilson, W.E., 1989. The effect of sampling duration on the ability to resolve source types using factor analysis. Atmos. Environ. 23, 239–254.

Liu, J., Mauzerall, D.L., Chen, Q., Zhang, Q., Song, Y., Peng, W., Klimont, Z., Qiu, X., Zhang, S., Hu, M., Lin, W., Smith, K.R., Zhu, T., 2016. Air pollutant emissions from Chinese households: a major and underappreciated ambient pollution source. Proc. Natl. Acad. Sci. U. S. A. 113 (28), 7756–7761 (2016).

Ma, Y., Cheng, Y., Qiu, X., Cao, G., Fang, Y., Wang, J., Zhu, T., Yu, J., Hu, D., 2018. Sources and oxidative potential of water-soluble humic-like substances ($HULIS_{WS}$) in fine particulate matter ($PM_{2.5}$) in Beijing. Atmos. Chem. Phys. 18, 5607–5617. https://doi.org/10.5194/acp-18-5607-2018.

Mao, J., Horowitz, L.W., Naik, V., Fan, S., Liu, J., Fiore, A.M., 2013. Sensitivity of tropospheric oxidants to biomass burning emissions: implications for radiative forcing. Geophys. Res. Lett. 40, 1241–1246. https://doi.org/10.1002/grl.50210 (2013b).

Marmur, A., Unal, A., Mulholland, J.A., Russell, A.G., 2005. Optimization based source apportionment of PM2.5 incorporating gas-to-particle ratios. Environ. Sci. Technol. 39, 3245–3254.

Marmur, A., Mulholland, J., Russell, A., 2007. Optimized variable source-profile approach for source apportionment. Atmos. Environ. 41, 493–505.

Nguyen, Q.T., Kristensen, T.B., Hansen, A.M.K., Skov, H., Bossi, R., Massling, A., Sørensen, L.L., Bilde, M., Glasius, M., Nøjgaard, J.K., 2014. Characterization of humic-like substances in Arctic aerosols. J. Geophys. Res. 119, 5011–5027.

Paatero, P., Eberly, S., Brown, S.G., Norris, G.A., 2014. Methods for estimating uncertainty in factor analytic solutions. Atmos. Meas. Tech. 7, 781–797.

Padoan, E., Amato, F., 2018. Vehicle non-exhaust emissions: impact on air quality. In: Amato, F. (Ed.), Non-exhaust Emissions: An Urban Air Quality Problem for Public Health, Impact and Mitigation Measures. Academic Press, London, pp. 21–65.

Polissar, A.V., Hopke, P.K., Paatero, P., Malm, W.C., Sisler, J.F., 1998. Atmospheric aerosol over Alaska 2. Elemental composition and sources. J. Geophys. Res. 103, 19045–19057.

Qiao, X., Ying, Q., Li, X., Zhang, H., Hu, J., Tang, Y., Chen, X., 2018. Source apportionment of $PM_{2.5}$ for 25 Chinese provincial capitals and municipalities using a source-oriented community multiscale air quality model. Sci. Total Environ. 612, 462–471.

Reuters, 2018. China to switch more households in central provinces to gas heating. Available from:. https://www.reuters.com/article/us-china-pollution-coal/china-to-switch-more-households-in-central-provinces-to-gas-heating-idUSKCN1N30Q8, Accessed date: 2 March 2019.

Salma, I., Ocskay, R., Chi, X.G., Maenhaut, W., 2007. Sampling artefacts, concentration and chemical composition of fine water-soluble organic carbon and humic-like substances in a continental urban atmospheric environment. Atmos. Environ. 41, 4106–4118.

Salma, I., Mészáros, T., Maenhaut, W., 2013. Mass size distribution of carbon in atmospheric humic-like substances and water soluble organic carbon for an urban environment. J. Aerosol Sci. 56, 53–60.

Shi, Z., Li, J., Huang, L., Wang, P., Wu, L., Ying, Q., Zhang, H., Lu, L., Liu, X., Liao, H., Hu, J., 2017. Source apportionment of fine particulate matter in China in 2013 using a source-oriented chemical transport model. Sci. Total Environ. 601, 1476–1487.

Song, J.Z., He, L.L., Peng, P.A., Zhao, J.P., Ma, S.X., 2012. Chemical and isotopic composition of humic-like substances (HULIS) in ambient aerosols in Guangzhou, South China. Aerosol Sci. Technol. 46, 533–546.

Squizzato, S., Masiol, M., Rich, D.Q., Hopke, P.K., 2018. A long-term source apportionment of $PM_{2.5}$ in New York State during 2005 to 2016. Atmos. Environ. 192, 35–47.

Srivastava, D., Tomaz, S., Favez, O., Lanzafame, G.M., Golly, B., Besombes, J.-L., Alleman, L.Y., Jaffrezo, J.-L., Jacob, V., Perraudin, E., Villenave, E., Albinet, A., 2018. Speciation of organic fraction does matter for source apportionment. Part 1: a one-year campaign in Grenoble (France). Sci. Total Environ. 624, 1598–1611.

Tan, J., Xiang, P., Zhou, X., Duan, J., Ma, Y., He, K., Cheng, Y., Yu, Z., Querol, X., 2016. Chemical characterization of humic-like substacnes (HULIS) in PM2.5 in Lanzhou, China. Sci. Total Environ. 573, 1481–1490.

Tao, J., Zhang, L.M., Zhang, R.J., Wu, Y.F., Zhang, Z.S., Zhang, X.L., et al., 2016. Uncertainty assessment of source attribution of $PM_{2.5}$ and its water-soluble organic carbon content using different biomass burning tracers in positive matrix factorization analysis - a case study in Beijing, China. Sci. Total Environ. 543, 326–335.

Uria-Tellaetxe, I., Carslaw, D.C., 2014. Conditional bivariate probability function for source identification. Environ. Model. Software 59, 1–9.

Varga, B., Kiss, G., Ganszky, I., Gelencser, A., Krivacsy, Z., 2001. Isolation of water-soluble organic matter from atmospheric aerosol. Talanta 55, 561–572.

Verma, V., Rico-Martinez, R., Kotra, N., King, L., Liu, J.M., Snell, T.W., Weber, R.J., 2012. Contribution of water-soluble and in-soluble components and their hydrophobic/hydrophilic sub-fractions to the reactive oxygen species-generating potential of fine ambient aerosols. Environ. Sci. Technol. 46, 11384–11392.

Voliotis, A., Prokes, R., Lammel, G., Samara, C., 2017. New insights on humic-like substances associated with wintertime urban aerosols from central and southern Europe: size-resolved chemical characterization and optical properties. Atmos. Environ. 166, 286–299.

Wang, B., Knopf, D.A., 2011. Heterogeneous ice nucleation on particles composed of humic-like substances impacted by O_3. J. Geophys. Res. 116, D03205.

Wang, H., Tian, M., Li, X., Chang, Q., Cao, J., Yang, F., Ma, Y., He, K., 2015. Chemical composition and light extinction contribution of PM2.5 in urban Beijing for a 1-year period. Aerosol Air Qual. Res. 15, 2200–2211.

Wang, D.S., Liu, M.R., Bai, X.F., Ding, H., 2016. The situation analysis of civil coal in the Beijing-Tianjin-Hebei region. Technology of Coal 3, 47–50 (in Chinese).

Wiedinmyer, C., Akagi, S.K., Yokelson, R.J., Emmons, L.K., Al-Saadi, J.A., Orlando, J.J., Soja, A.J., 2011. The Fire INventory from NCAR (FINN): a high resolution global model to estimate the emissions from open burning. Geosci. Model Dev. 4, 625–641. https://doi.org/10.5194/gmd-4-625-2011.

Xinhua, 2017. 126,000 Beijing households bid farewell to coal stoves in 2017. available at: . http://www.xinhuanet.com/english/2017-12/26/c_136853426.htm, Accessed date: 2 March 2019.

Xue, J., Yuan, Z.B., Yu, J.Z., Lau, A.K.H., 2014. An observation-based model for secondary inorganic aerosols. Aerosol Air Qual. Res. 14, 862–878.

Xue, J., Yuan, Z., Griffith, S.M., Yu, X., Lau, A.K., Yu, J.Z., 2016. Sulfate formation enhanced by a cocktail of high NO_x, SO_2, particulate matter, and droplet pH during haze-fog events in megacities in China: an observation-based modeling investigation. Environ. Sci. Technol. 50, 7325–7334.

Yu, L., Wang, G., Zhang, R., Zhang, L., Song, Y., Wu, B., Li, X., An, K., Chu, J., 2013. Characterization and source apportionment of PM2.5 in an urban environment in Beijing. Aerosol Air Qual. Res. 13, 574–583.

Zhang, R., Jing, J., Tao, J., Hsu, S.C., Wang, G., Cao, J., Lee, C.S.L., Zhu, L., Chen, Z., Zhao, Y., Shen, Z., 2013. Chemical characterization and source apportionment of $PM_{2.5}$ in Beijing: seasonal perspective. Atmos. Chem. Phys. 13, 7053–7074.

Zhang, Y., Cai, J., Wang, S., He, K., Zheng, M., 2017. Review of receptor-based source apportionment research of fine particulate matter and its challenges in China. Sci. Total Environ. 586, 917–929.

Zheng, M., Salmon, L.G., Schauer, J.J., Zeng, L., Kiang, C.S., Zhang, Y., Cass, G.R., 2005. Seasonal trends in PM2.5 source contributions in Beijing, China. Atmos. Environ. 39, 3967–3976.

Zheng, G.J., He, K.B., Duan, F.K., Cheng, Y., Ma, Y.L., 2013. Measurement of humic-like substances in aerosols: a review. Environ. Pollut. 181, 301–314.

Zíkova, N., Wang, Y., Yang, F., Li, X., Tian, M., Hopke, P.K., 2016. On the source contribution to Beijing $PM_{2.5}$ concentrations. Atmos. Environ. 134, 84–95.